Energy Proceedings
Vol 53, 2025
ISSN 2004-2965

Experimental and simulation study on thermal control performance of anisotropic CPCM#

Qun Liu[1], Hua Chen[1], Wen-Long Cheng[1*]

1 Department of Thermal Science and Energy Engineering, University of Science and Technology of China, Hefei, Anhui 230027, P. R. China

(Wen-Long Cheng: wlcheng@ustc.edu.cn)

ABSTRACT

Due to an incomplete understanding of the superior thermal control performance of anisotropic composite phase change materials (CPCMs) compared to isotropic CPCMs with equivalent thermal conductivity additives, this study delves into the thermal regulation capabilities of anisotropic CPCMs through experimental and numerical analyses. Through the compression method, CPCMs with varying anisotropy were synthesized for thermal control experiments. Under identical energy storage conditions, it was observed that the decrease in axial thermal conductivity has a greater inhibitory effect on the heat transfer rate than the promotion effect of radial thermal conductivity on it. The simulation analyzed anisotropic CPCM's thermal control on single and distributed heat sources in a constant space. It found that for single heat sources, there's a critical φ_{cv} factor. Above φ_{cv}, anisotropic CPCM outperforms isotropic. As thermal diffusion directions increase, CPCM thickness decreases, reducing φ_{cv}, while EG content minimally impacts φ_{cv}. For distributed heat sources, anisotropic CPCM offers superior temperature control by effectively mitigating temperature gradients between sources.

Keywords: anisotropy, isotropic, phase change materials, thermal control

NONMENCLATURE

Abbreviations	
CPCM	Composite phase change materials
EG	Expanded graphite
OBC	Olefin block copolymer
Symbols	
ΔH	Latent heat ($J \cdot kg^{-1}$)
k	Thermal conductivity ($W \cdot m^{-1} \cdot k^{-1}$)
T	Temperature (°C)
t	Time (s)
C_p	Specific heat ($J \cdot kg^{-1} \cdot K^{-1}$)
h	Convective heat transfer coefficient ($W \cdot m^{-2} \cdot K^{-1}$)
P	Preparation compression ratio
L	Length (mm)
d	Thickness (mm)
ρ	Density ($kg \cdot m^{-1}$)
φ	Thermal control size influence factor
δ	The distance between the heat source and the boundary (mm)
Subscripts	
x, y, z	x, y, z direction
sur	Ambient temperature
m	Melting
cv	Critical value

1. INTRODUCTION

With the highly integrated and complex development of electronic devices, there are problems of high local heat flux and uneven temperature distribution, which seriously affect the performance and lifespan of the devices[1]. Optimizing the application of heat dissipation systems and high-performance thermal interface materials is an effective means to alleviate heat accumulation. For narrow and limited space heat dissipation environments, the application of high-performance thermal interface materials is often more cost-effective[2]. In recent years, CPCMs, as a new type of passive thermal control interface material, have received widespread attention due to their advantages such as stable performance, safety and environmental protection, high energy storage density, and controllable space occupation[3]. CPCM efficiently mitigates heat accumulation in electronic devices by absorbing latent heat, while also safeguarding against instantaneous thermal shock damage and minimizing temperature fluctuations[4, 5]. Notably, flexible CPCM stands out for its excellent anti-leakage properties and ease of

This is a paper for the 16th International Conference on Applied Energy (ICAE2024), Sep. 1-5, 2024, Niigata, Japan.

installation, promising significant application potential in electronic thermal management[6].

Due to compact electronic packaging, the thermal interface CPCM's thickness is severely constrained, weakening its total heat capacity and reducing thermal storage, thereby compromising overall thermal management effectiveness. Researchers suggest utilizing thermal diffusion to mitigate the reduced total heat capacity issue from thin CPCM[7]. For effective heat transfer, CPCM must exhibit high thermal conductivity along the heat transfer direction. Anisotropic CPCM offers high conductivity in a specific direction with fewer thermal conductive additives[8]. Various methods for preparing anisotropic CPCM include directional freezing, self-assembly techniques, shear induction, and compression methods[8-10]. Among the four methods, the compression approach stands out for its simplicity of operation and flexibility in adjusting material dimensions. At present, multiple studies have been devoted to the preparation of anisotropic CPCM and the establishment of thermal conductivity prediction models, but few studies are exploring the improvement of the thermal control effect of anisotropic CPCM compared to isotropic CPCM, leaving a research gap.

Therefore, this study used compression technology to develop an anisotropic CPCM, evaluating its thermal management in experiments. To gain a deeper understanding and quantify the advantages of this material over isotropic CPCM in thermal control, we employed finite element simulation technology and conducted a detailed analysis and comparison using our team's previously established CPCM thermal conductivity prediction model. This systematically revealed the significant performance of anisotropic CPCM in improving thermal control effectiveness.

2. ANISOTROPIC CPCM THERMAL CONTROL EXPERIMENT

2.1 Material preparation and thermal properties

The anisotropic CPCM, composed of paraffin, OBC, and expanded graphite in a 79:16:5 ratio, is prepared by mixing paraffin and OBC in a high-temperature stirred tank at 160°C for 30 mins, followed by adding EG and stirring under vacuum for 1 h. After hot-pressing, the mixture forms the initial CPCM. Further compression enhances anisotropy. Thermal performance and test results are presented in Table 1 and Fig. 1(b).

Table 1 Thermal properties of anisotropic CPCM

Thermal property	Value
Phase change peak temperature (°C)	44
Latent heat (kJ·kg^{-1})	172.8
Density (kg·m^{-3})	922
Specific heat capacity (J·kg^{-1}·K^{-1})	2174

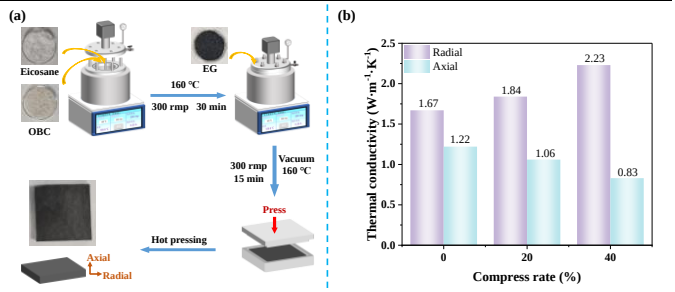

Fig. 1 (a) Preparation process of anisotropic CPCM and (b) anisotropic thermal conductivity of CPCM

2.2 Experimental setup and uncertainty analysis

The thermal control experimental setup for anisotropic CPCMs is displayed in Fig. 2. It comprises a silica gel heater, anisotropic CPCM, cover plates, insulation foam, and bolts. The heating element is centered below the CPCM, compressed by cover plates, and fixed with bolts. Insulation foam prevents heat loss. The ambient temp is 25 °C. The experimental outcomes are displayed as temperature, with measurement errors stemming primarily from the thermocouple (±0.4%) and Agilent data acquisition instrument (±0.08%), yielding a total error of approximately 0.408%.

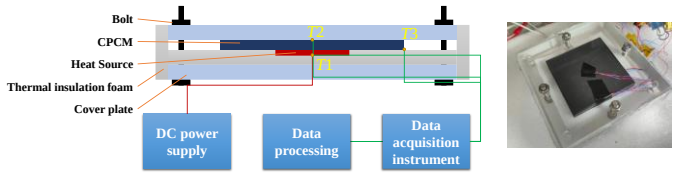

Fig.2 Physical and schematic diagrams of the experimental setup

2.3 Thermal control experiment results

To bolster the credibility of our experimental findings, we conducted thermal control tests on an identical material, subjecting it to varying levels of compression. As depicted in Fig. 3, with rising compression ratios, the heat source's center temperature and both axial and radial temperature disparities intensify. This trend arises due to the material's increased radial thermal conductivity and decreased axial conductivity under compression, facilitating radial heat flow and hindering axial thermal transfer. However, under the same CPCM energy storage, the decrease in axial (normal) thermal conductivity has a greater inhibitory effect on the heat transfer rate than the promotion effect of radial (circumferential) thermal conductivity on the heat

transfer rate, resulting in a decrease in the overall rate of heat conduction in the CPCM and an increase in the center temperature of the heat source. In addition, although reducing the thickness of CPCM is beneficial for reducing axial temperature difference, the decrease in heat transfer rate caused by the decrease in axial thermal conductivity is more pronounced, resulting in an increase in axial temperature difference of PCM with the increase of compression ratio. The increase in radial temperature difference of CPCM is mainly due to the increase in lateral size of CPCM after compression. The test results are similar for compression ratios of 0 and 20%, potentially attributed to the reduction in surface roughness and contact thermal resistance with the heat source after secondary compression, resulting in improved heat transfer. This experimental result can also be used to confirm that the heat transfer effect of CPCM decreases with increasing compression in the presence of compression.

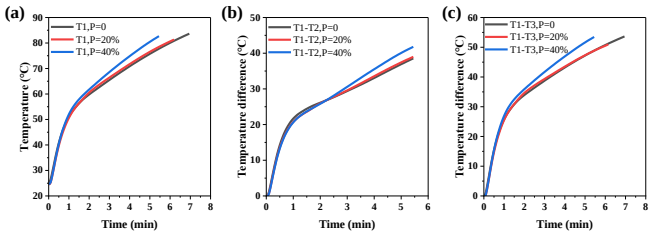

Fig. 3 Thermal control effect of anisotropic CPCM

3. NUMERICAL MODELING OF ANISOTROPIC CPCM THERMAL CONTROL

3.1 Physical Models and Numerical Methods

To better explore the anisotropic materials' thermal control capabilities across various scenarios (Fig. 4), three models were devised: the circumferential heat transfer model and the bidirectional heat transfer model under a single heat source, as well as the heat transfer model under a distributed heat source. In practical applications, the thermal control space is typically fixed, so when changing the anisotropic thermal conductivity of CPCM in the simulation model, the CPCM's thickness is kept consistent. In practical applications, the thermal control space is typically fixed, necessitating the maintenance of CPCM's thickness while altering its anisotropic thermal conductivity in simulation models. The size of the heat source in the model is 20×20×2 mm^3. The thickness of the cover plate and insulation material is 2.5 mm and 2 mm respectively, and their circumferential dimensions are the same as CPCM. To streamline the model, we adopted the following assumptions: (1) Thermal conduction is the sole heat transfer mechanism; (2) The density and thermal conductivity of CPCM remain constant throughout the phase transition; (3) Radiative heat transfer is disregarded; (4) Material deformation under compression does not alter its density.

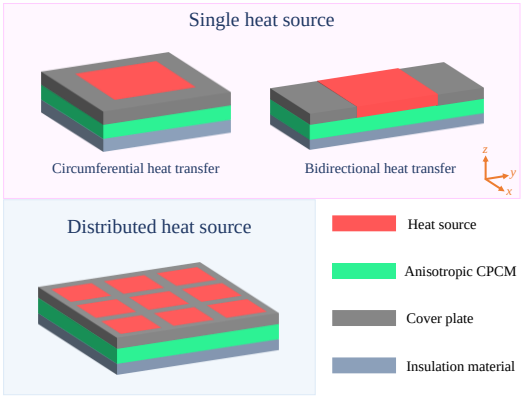

Fig. 4 Thermal Control Simulation Model

Based on the above assumptions, the control equation of the model is:

$$\rho C_{\mathrm{p}} \frac{\partial T}{\partial t} = k_x \frac{\partial^2 T}{\partial x^2} + k_y \frac{\partial^2 T}{\partial y^2} + k_z \frac{\partial^2 T}{\partial z^2} \tag{1}$$

Where k_x, k_y, k_z are the thermal conductivity of the material in the x, y, and z directions, ρ is the density of the material, C_{p} is the specific heat capacity of the material. The converted heat capacity in the phase change region is written as follows[6]:

$$C_{\mathrm{eff,\,CPCM}}(T) = C_{\mathrm{p,\,CPCM}} + \delta(T)\Delta H \tag{2}$$

Where $C_{\mathrm{p,CPCM}}$ is the specific heat capacity of anisotropic CPCM in the non-phase transition range, ΔH is the latent heat of phase transition of anisotropic FCPCM, and $\delta(T)$ is the Gaussian distribution function.

$$\delta(T) = \frac{\exp\left(-\left(T-T_{\mathrm{m}}\right)^2/\left(\Delta T\right)^2\right)}{\Delta T\sqrt{\pi}} = N\left(T_{\mathrm{m}}, \frac{\Delta T}{\sqrt{2}}\right) \tag{3}$$

The theoretical density, theoretical specific heat capacity, and theoretical latent heat of CPCM under different EG contents can be calculated using the following formula:

$$\rho_{\mathrm{CPCM}} = \rho_{\mathrm{OBC}}\omega_{\mathrm{OBC}} + \rho_{\mathrm{PA}}\omega_{\mathrm{PA}} + \rho_{\mathrm{EG}}\omega_{\mathrm{EG}} \tag{4}$$

$$C_{\mathrm{p,\,CPCM}} = C_{\mathrm{p,\,OBC}}\omega_{\mathrm{OBC}} + C_{\mathrm{p,\,PA}}\omega_{\mathrm{PA}} + C_{\mathrm{p,\,EG}}\omega_{\mathrm{EG}} \tag{5}$$

$$\Delta H_{\mathrm{CPCM}} = \Delta H_{\mathrm{PA}}\omega_{\mathrm{PA}} \tag{6}$$

Where ω is the quality score. The lower side of the cover plate is subject to air convection.

$$-k\frac{\partial T}{\partial z} = h\left(T - T_{\mathrm{sur}}\right) \tag{7}$$

Where h is the convective heat transfer coefficient, and T_{sur} is the ambient temperature.

To enhance the practicality of this study's discussion outcomes, the anisotropic thermal conductivity of CPCM

was input using the anisotropic thermal conductivity model of CPCM under compression conditions previously established by our research team. Given the consistency in materials and preparation methods with prior works, the pertinent prediction methodologies and parameters are comprehensively outlined in the referenced literature[9]. Among them, to better compare the thermal control effects of anisotropic and isotropic CPCM under the same content of EG, the initial compression rate P_0 in the prediction parameters was set to 0, and the prediction results are shown in Fig. 5.

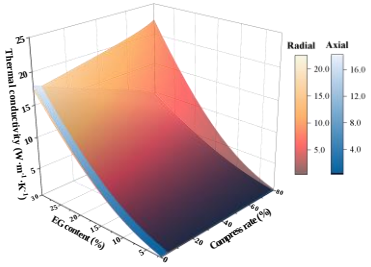

Fig. 5 Predicted Thermal Conductivity of CPCM

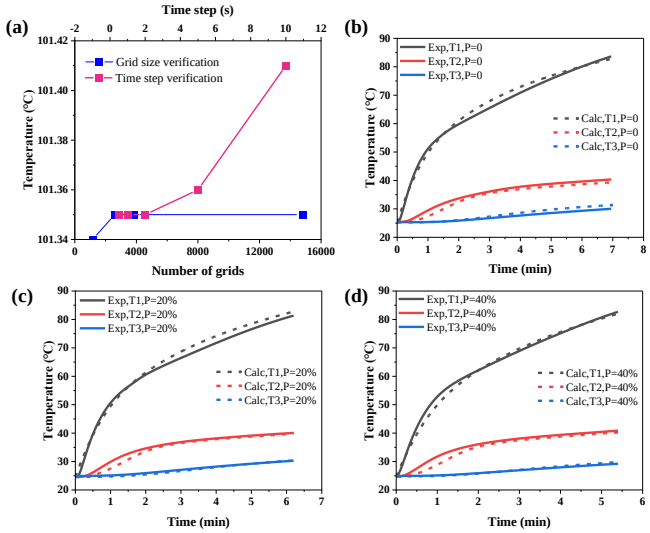

Fig. 6 Independence Test (a) and Model Validation (b-c)

3.2 Independence testing and model validation

The grid independence verification employed four grid sizes: 1152, 2592, 3872, and 14792, equivalent to maximum grid values of 4 mm, 2.5 mm, 2 mm, and 1 mm, respectively. Irrespective of the grid used, a consistent temperature rise pattern emerged. To determine the optimal grid size, we referenced the heat source temperature at 1000 s. Fig. 6(a) indicates that temperatures stabilize beyond the 2.5 mm grid size. Hence, 2.5 mm was chosen for subsequent analyses. Similarly, evaluating calculation step sizes (0.5 s, 1 s, 2 s, 5 s 10 s) using the same criterion revealed stability below or at 2 s. Thus, 2 s was adopted as the calculation step size. Moreover, Fig. 6(b)-(c) showcases a close alignment between experimental and simulation results, underscoring the simulation model's reliability.

4. THERMAL CONTROL THEORY ANALYSIS OF ANISOTROPIC CPCM

4.1 Thermal control effect of anisotropic CPCM under single heat source

Due to the compression method used in this study to prepare anisotropic CPCM, CPCM with larger dimensions in the direction of high thermal conductivity is easier to prepare. Therefore, $k_x=k_y>k_z$ is set in the model. The simulation in this section uses a single heat source circumferential expansion model, with a CPCM thickness of 3 mm, a heat source heating power of 3 W, and an EG addition of 10% in the CPCM. Referring to the safe operating temperature of electronic devices, it is assumed in the analysis that the upper limit of the working temperature of the heat source is 80 °C. The thermal control size factor φ for anisotropic CPCM is defined as the ratio of thermal diffusion size in the x or y direction to PCM thickness, as specified in Eq. (8).

$$\varphi = \frac{L_{\mathrm{PCM}} - L_{\mathrm{chip}}}{d_{\mathrm{PCM}}} \tag{8}$$

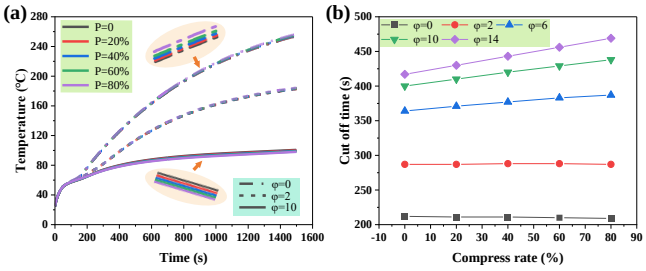

Fig. 7 The thermal control effect of anisotropic CPCM on heat sources under different diameters. (a) Heating rate of heat source; (b) The thermal control time of CPCM.

Where L_{pcm}, L_{chip}, and d_{pcm} are the dimensions of PCM thermal diffusion direction, heating element size, and PCM thickness, respectively. As depicted in Fig. 7, when φ=0 and the CPCM's compression (P) increases, the thermal control efficacy diminishes, causing the heat source's upper-temperature limit to be reached sooner. This occurs because the CPCM's circumference equals the heat source's, restricting circumferential heat diffusion to solely z-direction transfer, where k_z prevails. Higher CPCM compression rates lead to reduced z-direction thermal conductivity, subsequently lowering the heat transfer rate. When φ=2, both anisotropic and isotropic CPCM exhibit similar thermal control, with identical safe operation temperature control times. When φ>2, anisotropic CPCM outperforms isotropic

CPCM, with increased anisotropy lengthening and enhancing thermal control time for the heat source. Thus, φ=2 represents the critical φ_{cv} value for anisotropic CPCM under these conditions. When $\varphi<\varphi_{cv}$, longitudinal thermal conductivity decline significantly reduces heat transfer, so choosing isotropic CPCM is better. On the contrary, when $\varphi>\varphi_{cv}$, the increase in heat transfer efficiency caused by the increase in transverse thermal conductivity dominates, hence anisotropic CPCM is preferable. Fig. 7(b) further shows that the larger φ is, the more obvious the enhancement of the heat transfer effect brought by anisotropy is.

4.2 Factors affecting thermal control of anisotropic CPCM under single heat source

CPCM thickness and expansion direction. From Fig. 8(a), it is evident that the φ_{cv} values, for both the circumferential and bidirectional heat transfer models rise with increased CPCM thickness, accompanied by an accelerating trend in the growth of φ_{cv}. This is because the thicker the CPCM, the more important the normal heat transfer, and the decrease in heat transfer efficiency caused by the decrease in k_z thermal conductivity has a more significant impact on the overall thermal control effect. Furthermore, the φ_{cv} of the circumferential heat transfer model is lower than that of the bidirectional model, with a slower rate of increase with CPCM thickness. This is attributed to the multiple heat diffusion directions in the circumferential model, facilitating a quicker enhancement of heat transfer. Fig. 8(b) illustrates the thermal control effect of CPCM (50 mm length, 10% EG) varying with thickness. Anisotropic CPCM exhibits superior thermal control compared to isotropic CPCM. At an 80% compression rate and 3mm thickness, CPCM achieves a max elongation rate of 9.5%. Moreover, due to the decline in heat transfer efficiency reduced normal thermal conductivity positively correlates with thickness, as CPCM thickness reaches 6mm, the time to attain 80°C initially rises before declining.

EG content. Fig. 8(c) reveals that for anisotropic CPCM, φ_{cv} remains nearly constant when EG content exceeds 10%, suggesting a minimal correlation between φ_{cv} and EG content in this range. But at 5% EG content, the φ_{cv} is larger. Because when the EG content is low, the limited boost in radial thermal conductivity with compression results in minimal heat transfer enhancement and does not significantly prolong the thermal control time (Fig.8 (d)). when EG content is 5%, radial thermal conductivity increases by only 0.23 $W \cdot m^{-1} \cdot K^{-1}$ with compression (0-80%), while axial thermal conductivity decreases by 0.46 $W \cdot m^{-1} \cdot K^{-1}$. Fig. 8(d) indicates that increased EG content enhances temperature control under identical CPCM size, with anisotropic CPCM outperforming isotropic CPCM in thermal regulation. However, beyond 20% EG, further additions or anisotropy yield insignificant thermal control gains. This is because the heat transfer process within the PCM is already relatively efficient at this stage, and additional increases in thermal conductivity have a limited impact on improving heat transfer efficiency.

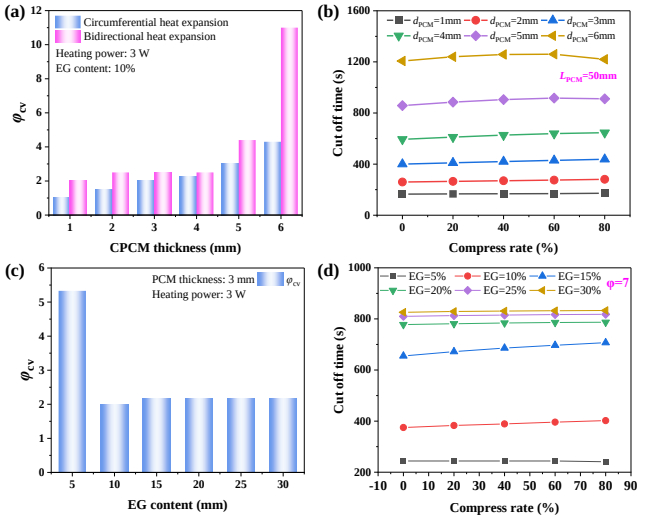

Fig. 8 (a) φ_{cv} of CPCM at different thicknesses and thermal diffusion directions; (b) thermal control time of CPCM on heat sources; φ_{cv} (c) and thermal control time (d) of CPCM at different EG contents for the heat source.

4.3 The thermal control effect of anisotropic materials on distributed heat sources

This section investigates the thermal control effect of anisotropic CPCM with 10% EG content on distributed heat sources. The CPCM thickness is 3 mm, and each heat source has a heating power of 3 W. The distance between heat sources is set to twice the distance between the heat source and the boundary (δ). This section examines the cases where δ is 1.5 mm and 10.5 mm, corresponding to combinations of 9 single heat source circumferential models with φ values of 1 and 7, respectively. Fig. 9 shows that in both cases, the thermal control effect of CPCM on distributed heat sources improves with increased preparation compression. As the preparation compression amount increases, the minimum temperature of the heat source rises, while the maximum temperature decreases. Consequently, the temperature difference between the heat sources decreases with increased preparation compression. This is because the circumferential thermal conductivity of CPCM is enhanced with greater preparation

compression, allowing for better temperature balance among the heat sources. Therefore, when dealing with distributed heat sources, selecting anisotropic materials for thermal control yields superior results compared to the single heat source circumferential model mentioned earlier.

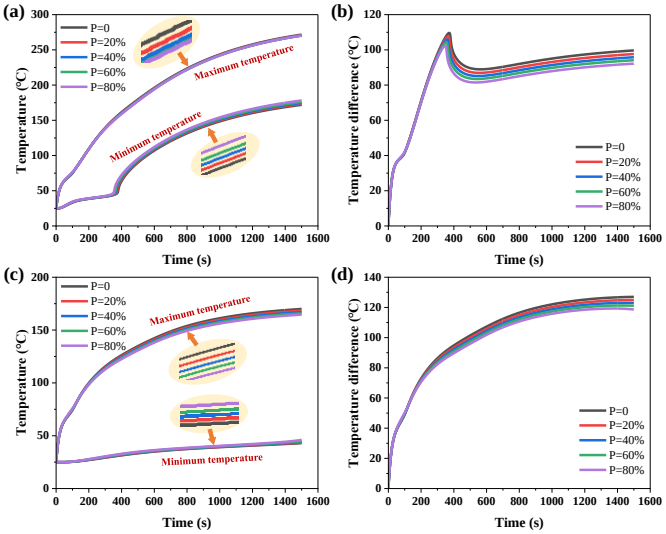

Fig. 9. The maximum temperature, minimum temperature, and temperature difference of the heat source for L values of 1.5 mm (a-b) and 10.5 mm (c-d)

5. CONCLUSIONS

This study examines the thermal control efficacy of anisotropic CPCM via experiments and simulations. Anisotropic CPCM was prepared using the compression method. The experimental results show that under the same energy storage, the inhibitory effect of the decrease in axial (normal) thermal conductivity on the heat transfer rate exceeds the promoting effect of the increase in radial (circumferential) thermal conductivity on the heat transfer rate. The simulation assessed anisotropic CPCM's thermal control for single and distributed heat sources in a constant space. The results indicate that for single heat sources, there's a critical φ_{cv} factor. When $\varphi>\varphi_{cv}$, choosing anisotropic CPCM has a better thermal control effect than isotropic CPCM; When $\varphi\leq\varphi_{cv}$, choosing isotropic CPCM is better. The more directions of thermal diffusion, the thinner the CPCM, and the smaller the φ_{cv}. The EG content has little effect on φ_{cv}. However, excessive or insufficient EG content limits anisotropic CPCM's thermal control enhancement, making isotropic CPCM a viable alternative. For distributed sources, anisotropic CPCM excels in minimizing temperature disparities, offering superior temperature control.

ACKNOWLEDGEMENT

This work was supported by the National Key R&D Program of China (Grant No. 2022YFC2204403).

REFERENCE

[1] He ZQ, Yan YF, Zhang ZE. Thermal management and temperature uniformity enhancement of electronic devices by micro heat sinks: A review. Energy. 2021;216:119223.

[2] Zhao CG, Li YF, Liu YC, Xie HQ, Yu W. A critical review of the preparation strategies of thermally conductive and electrically insulating polymeric materials and their applications in heat dissipation of electronic devices. Adv Compos Hybrid Mater. 2023;6(1):27.

[3] Zhang S, Feng DL, Shi L, Wang L, Jin YG, Tian LM, et al. A review of phase change heat transfer in shape-stabilized phase change materials (ss-PCMs) based on porous supports for thermal energy storage. Renew Sust Energ Rev. 2021;135:110127.

[4] Kang J-H, Deng Q, Liu H-J, Chen H, Zhao R, Yang C-P, et al. Study on Temperature Noise Suppression Characteristics Based on Multilayer Composite Structure. International Journal of Thermophysics. 2024;45(8):109.

[5] Liu Q, Deng Q, Zhao R, Cheng WL, Wang YD. A novel flexible flame-retardant phase change materials with battery thermal management test. Journal of energy storage. 2023;70:108077.

[6] Huang YH, Cheng WL, Zhao R. Thermal management of Li-ion battery pack with the application of flexible form-stable composite phase change materials. Energy Convers Manag. 2019;182:9-20.

[7] Li WW, Wang F, Cheng WL, Chen X, Zhao Q. Study of using enhanced heat-transfer flexible phase change material film in thermal management of compact electronic device. Energy Convers Manag. 2020;210:112680.

[8] Wu Y, An C, Guo Y, Zong YY, Jiang NS, Zheng QB, et al. Highly Aligned Graphene Aerogels for Multifunctional Composites. Nano-Micro Letters. 2024;16(1):118.

[9] Mao LK, Liu Q, Chen H, Cheng WL. A novel model of the anisotropic thermal conductivity of composite phase change materials under compression. Int J Heat Mass Transf. 2024;227:125512.

[10] Mao LK, Zhao R, Chen J, Cheng WL. Theoretical and experimental study on the anisotropic thermal conductivity of composite phase change materials prepared by hot-pressing method. Int J Heat Mass Transf. 2022;198:123380.